Radargrammetric Measurements from the Initial Magellan Coverage of Planet Venus

Franz W. Leberl, Kelly Maurice, John Thomas, and *Wolfgang Kober*
Vexcel Corporation, 2477 55th Street, Boulder, CO 80301

ABSTRACT: In August/September 1990, NASA's Magellan Mission to planet Venus began to image the planet's surface with the help of a Synthetic Aperture Radar system. By May 1991 the initial coverage of the surface of the entire planet was completed in 1789 orbits. Due to gaps, these orbits produced about 1,650 image strips covering 84 percent of the planet's surface. Each orbit resulted in an image strip of a width of 350 pixels and a length of more than 220,000 pixels. Each orbit also resulted in an altimeter trace with a variable instantaneous footprint of about 10 to 30 km in diameter, and radiometry observations with footprints of about 80 km, using the same radar system to obtain these three data sets.

The orbit and imaging geometry produce a coverage with single image strips which does limit one's analysis to two dimensions only; the third dimension, terrain elevation, is usually not available from such data. We did attempt, however, to assess a few non-traditional techniques of surface elevation measurements to report on terrain slopes and the elevation of specific terrain features.

Single image three-dimensional measurements are based on the assumption that certain features are symmetric, and employ slope information obtainable from shape-from-shading or radar clinometry. We describe the available techniques and assess their accuracy. We illustrate the topographic elevation measurements with a data set of the impact crater Danilova (26.4°S, 337.2°E), which we confirm to have a rim height of 1,560 metres, with an uncertainty of ±200 metres. We use this data set to also illustrate the shape-reconstruction from shading and apply this technique to an area at 83°N, 335°E.

THE MAGELLAN MISSION TO PLANET VENUS

THE NOMINAL MAGELLAN MISSION TO PLANET VENUS was completed on 15 May 1991, after 243 days of continuous mapping with the Synthetic Aperture Radar (SAR), altimeter, and passive radiometer, all based on the same radar system and multiplexing three types of measurements (see Table 1). The result of the nominal mission is an unprecedented volume of 1,650 images of a length of about 17,000 km and width of 20 km. Planet Venus has about the same radius as the Earth, and coverage of Venus is thus comparable to covering the Earth. Considering that there is no ocean on Venus, the land mass to be imaged is much greater on Venus than it is on Earth. Given the fact that radar image coverage of the Earth is minimal at this time, Magellan results in a data set that is unique for any planet; Earth is still waiting to be imaged in this manner.

Each image consists of 350 by 220,000 pixels of a diameter of 75 metres denoted as Full Resolution Basic Image Data Record, or F-BIDR (and also as "noodles"). From this source material numerous data products are currently being generated in the form of traditional image maps at various scales and covering the entire planet. These are denoted by acronyms such as F- or C-MIDR (Full Resolution or Compressed Resolution Mosaicked Image Data Record), useful for presentation at scales of 1:300,000 and smaller. Figure 1 shows a well-publicized area denoted as the "crater farm." A subarea from this mosaic will be the focus of subsequent studies in this paper (Figure 2).

Considerable scientific publicity has been generated by this mission and its initial scientific results (Science, 1991; Saunders, 1990). Some key parameters are described in Table 1. The mission now continues into a so-called Cycle 2, generating a second complete coverage of the planet's surface at a different imaging geometry, looking at the surface from an opposite side (namely right-looking), with a look angle of about 25°, whereas the initial Cycle 1 coverage was left-looking at a variable look angle between 43° and 10° . This Cycle 2 may then be followed by a third coverage and possibly produce a complete stereo-usable same-side (left-looking) coverage when combined with the initial coverage.

MAPPING PRODUCTS

The basis for the development of systematic mapping products from Magellan initially consists of historical altimeter measurements to describe the surface elevations, obtained from Pioneer-Venus and Venera. As new Magellan altimetry data become available, these may be employed as a basis for future map processing. The raw altimetry measurements have a spacing of about 20 km across orbits (at periapsis) and are denser near the poles. The spacing along each orbit is about 8 km. The accuracy of this digital elevation model (DEM) depends on the ruggedness of the terrain, as we will discuss later. In spite of a range measurement accuracy of up to ±5 metres, significant elevation errors can be made in mountainous areas, in excess of a kilometre, due to the horizontal ambiguity in deciding which surface point gave rise to the shortest slant range measurement or the maximum of the echo function.

The raw SAR echoes are so-called phase histories; they are received at the antennas of NASA's Deep Space Network, brought to the Jet Propulsion Laboratory, and converted to image pixels. These pixels form raw images that are rectified with the measurements of the satellite positions in a process denoted as *dead-reckoning*. Each pixel representing an image point is projected onto the surface developed from an altimeter, thereby using the ephemeris data for the satellite as computed by the satellite navigation team. Rectified individual radar image strips are expected to match at the seams at a given presentation scale. The geometric transformations used for dead-reckoning are being stored in one of the header files of each F-BIDR and are thus available to reconvert the delivered basic image strips into Doppler frequencies and range measurements for radargrammetric applications, thereby defining a projection circle in three-dimensional space as the locus of the object point (for a discussion of radargrammetry, see the radargrammetric literature, e.g., Leberl (1990)).

Image rectification and reformatting into mosaicked products are an activity of the Mission. These products are being distributed to the scientific community in the form of photographic representations of the mosaics, or in the form of CD-ROMs for

PHOTOGRAMMETRIC ENGINEERING & REMOTE SENSING,
Vol. 57, No. 12, December 1991, pp. 1561–1570.

0099-1112/91/5712–1561$03.00/0

TABLE 1. KEY PARAMETERS OF THE MAGELLAN MISSION, RADAR IMAGING SYSTEM, AND HISTORICAL VENUS RADAR DATA

Mission:	
Date of launch from Kennedy Space Center, Florida	4 May 1989
Date of Venus orbit insertion	10 August 1990
Beginning of systematic radar imaging	15 September 1990
Completion of initial coverage (all 360°, Cycle 1)	15 May 1991
Completion of second coverage (Cycle 2)	14 January 1992
Orbit inclination	85°
Spacecraft altitude above surface at periapsis	294 km
Spacecraft altitude above surface at apoapsis	8458 km
Radar Imaging:	
Width of radar image strip (and angular width of beam)	20 km (2.5°)
Length of radar image strip	17,000 km
Radar image pixel size	75 m by 75 m
Radar image range resolution	88 m (0.59μsec)
Radar image azimuth resolution at 5 to 17 looks per pixel	120 m
Spacecraft altitude above surface at beginning of strip	2,225 km
Geographic latitude at beginning of each radar image	90°North
Look angle off-nadir at beginning of each radar image	11°
Geographic latitude at periapsis	9.9°North
Maximum look angle off-nadir (at periapsis)	43°
Radar wavelength	12.6 cm
Angular width of image at antenna, at periapsis and 80°N	2° and 0.5°
Radar image overlaps at 80° North	18 km
Radar image stereo intersection angles at 80°North	0.1°
Altimetry:	
Footprint varies with S/C altitude from	10 by 12 km² to 20 by 29 km²
Spacing of footprints along orbit	8 km, more at Pole
Error of altimetric elevations, exclusive of orbit errors	> 5 meters
Passive Radiometry:	
Footprint varies with S/C altitude from	16 by 24 km² to 83 by 87 km²
Sampling interval	5 km by Swath Width
Previous Imaging Data of the Surface of Planet Venus:	
Pioneer Venus	1978–1981
Radiometry at Resolution of	200 to 800 km
Altimetry with spacing of measurements (along by across)	120 km by 150 km
Radar reflectivity measurements (radar imaging)	30 km pixels, 8 pixels/swath
Radar look angle off-nadir at periapsis	15° to 65°
Wavelength	17 cm
Venera 15 and 16:	1983–1984
Radar imaging with pixel size	0.8 km
Range resolution	1.5 km
Wavelength	8 cm
Radar look angle off-nadir	10°
Earth based radar imaging (near 0° incidence angle)	Since 1964
Wavelength	12.6 cm
Arecibo antenna, Puerto Rico	1–2 km
Goldstone (California) and other antennas	2–3 km

use in the analyst's digital image processing systems. Table 2 describes relevant data products. Mosaics are simply composed of image strips that were individually rectified with the beforementioned dead-reckoning method.

The ability to take advantage of the image overlaps exists: one could pick tie points between adjacent image strips and refine the matching between mosaicked images. However, cost prevents this approach from being used routinely, and the reduced resolution mosaics are well within the desired accuracy so that tie point identification would not be justified. Tie point identification is, however, employed in two specific tasks near the pole. In order to determine the location of the pole, and to refine the computation of the ephemeris, polar images are tied together by tie-points and subjected to an image block adjustment (Davis, personal communication, 1991; Chodas, personal communication, 1991).

THREE-DIMENSIONAL MAPPING

The ability to extract three-dimensional measurements of local surface elevations from initial mission data is limited to altimetry. This results in a coarse digital elevation model (DEM), but for the surface of the entire planet (Pettengill *et al.*, 1991). A sample area for crater Danilova is reproduced in Figure 3a and covers an area of 77 km by 77 km. The DEM postings are interpolated at regular intervals of 4.641 km and distributed as the Global Topographic Data Record (GTDR). Figure 3b combines the DEM with the radar image coverage and seems to confirm that the altimetry DEM in the form of the GTDR represents a high-pass filtered version of the crater.

Of course, as one examines surface phenomena more closely, immediate questions concern the height of volcanoes, depth of craters, slope of certain terrains, etc. This could be measured if a stereo coverage were available, or if interferometric measurements were feasible, or if the altimeter had a narrow footprint. Table 3 summarizes the range of radar techniques that are in principle capable of determining the three-dimensional elevation differences on a planetary surface. It becomes quickly evident that the initial Magellan imagery will not permit the development of a systematic contour map with a resolution that is higher than that of the altimeter.

The only method that could potentially produce a detailed elevation map from Cycle 1 imagery, with postings at every pixel, is shape-from-shading. Given uniform surface properties, this technique is capable of developing a map of slope changes and it will create a DEM that will describe relative elevations (Thomas *et al.*, 1991). It may, however, be very sensitive to errors in assumed electric properties of the surface, resulting in a scaling problem and in potentially significant absolute elevation errors.

We will describe in the following several techniques to obtain elevation measurements from the initial single image coverage of Venus, and we will assess their accuracies. We select the image of crater Danilova as a representative study area (see Figures 1 through 3), and we will show that this crater has a depth of 1,560 metres, with an uncertainty in the range of about ±200 metres.

ELEVATION MEASUREMENT TECHNIQUES

ALTIMETRY

The most direct method to measure terrain elevations is of course with an altimeter. Figure 3 described one of several products one can obtain from Magellan's altimeter. This is the result of interpolating a regular square grid from input postings computed from individual altimeter footprints. Figure 4 is an example of such footprints, each of which can be related to a specific area on the planet, as indicated in Figure 5.

In their routine application the altimetry data may not be

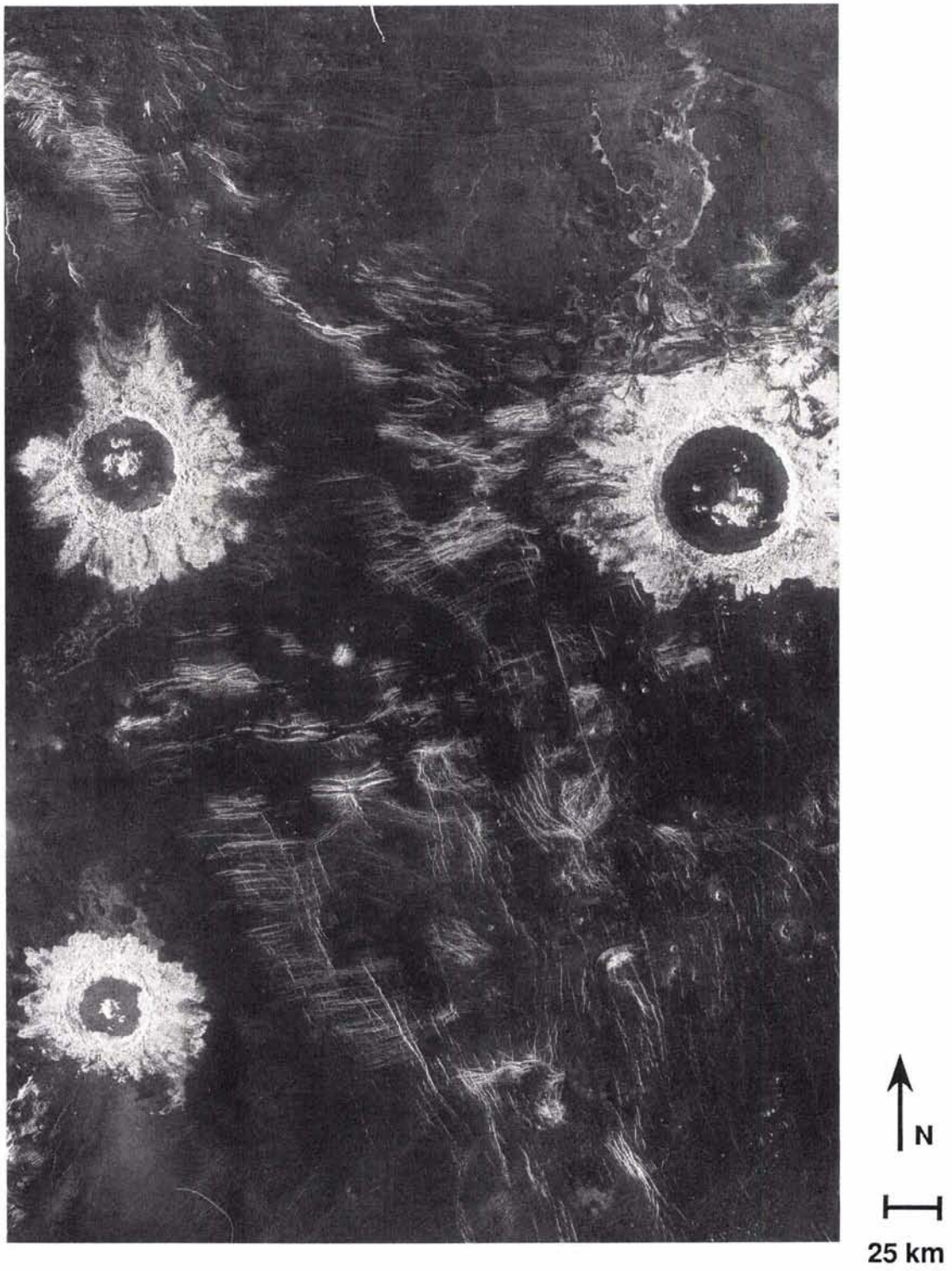

FIG. 1. Mosaicked imaging product of the crater farm at 27°S, 339°E. This is a partial F-MIDR covering a width of 300 km and consisting of 23 orbits. At 8 pixels per millimetre, this lends itself for presentation at a Scale 1: 600,000. The northwestern-most crater (above left) is Danilova and subject to analysis in this report.

capable of resolving an individual crater, so that the rim and floor may not get observed separately. However, some information about crater depth may be present in the so-called echo functions. Figure 6 illustrates an example from footprint B in Figure 4: in it we can discern several strong echoes and conclude that they result from reflections off the crater rim and crater floor. If this interpretation is correct, then we can measure the crater depth by the distance in range between echo-peaks. We

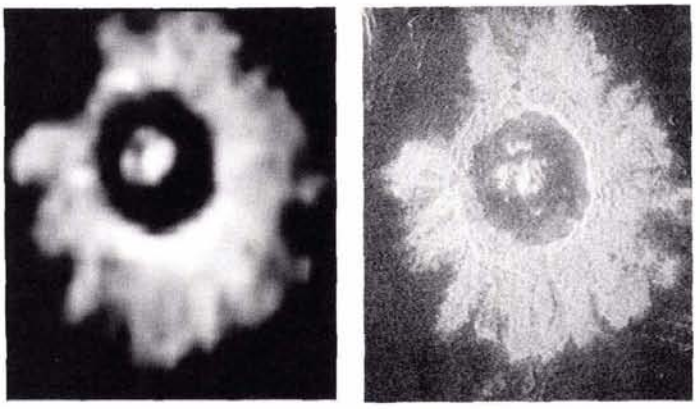

(a) Arecibo Image (b) Magellan Image

FIG. 2. (a) Image of Crater Danilova from Earth-based Radar, Arecibo, Puerto Rico, resampled from approximately 4,000-m to 300-m resolution. (b) Image of Crater Danilova from Magellan, resampled from 75-m to 300-m resolution. Note the increase in detail shown in the Magellan image over the Arecibo image.

TABLE 2. MAJOR DATA PRODUCTS FROM THE NOMINAL MAGELLAN MISSION, TO BE AVAILABLE FROM THE NATIONAL SPACE SCIENCE DATA CENTER AT GREENBELT, MARYLAND

Name	Description	Pixel	Comment
F-BIDR	Full resolution Basic image data record	75 m	100MB per orbit
F-MIDR	Full resolution Mosaicked image data record	75 m	5° by 5°, 530 by 530 km²
C1-MIDR	Compressed once Mosaicked ...	225 m	15° by 15°
C2-MIDR	Compressed twice Mosaicked	675 m	45° by 45°
C3-MIDR	Compressed thrice...	2025 m	120° by 120°
ARCDR	Altimetry and radiometry composite data record		Individual echoes
GTDR	Global topography data record	5 km	Global, interpolated and filtered from ARCDR
GSDR	Global slope data record	5 km	From altimetry echoes
GREDR	Global reflectivity data record	5 km	From altimetry echoes
GEDR	Global emissivity data record	5 km	From radiometer mode

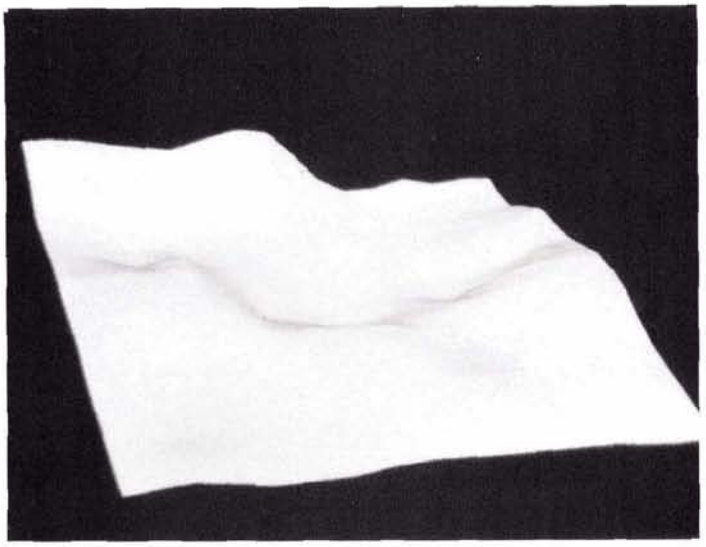

(a) DEM only

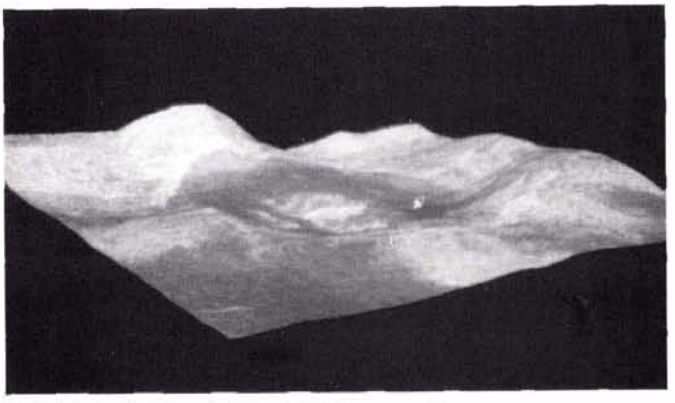

(b) DEM with image overlay

FIG. 3. (a) Small segment of a digital elevation model (DEM) obtained from Magellan's altimeter. Made available by G. Pettengill and P. Ford, MIT (see Pettengill *et al.*, 1991). The DEM is displayed with 150-m pixels. These result from densifying the GTDR data which provide a DEM point at a 4.5-km spacing. Area is 77 km by 77 km. Compare with Figure 3(b) to relate the crater to the DEM. (b) Same as (a), but with the radar image mosaic superimposed over the DEM. Center is at 26.4°S, 337.2°E.

can repeat such a measurement in all those footprints that cover both the rim and crater floor, and obtain redundant observations for the single value of crater depth.[1] However, to accomplish this we need the image to interpret the echo functions meaningfully.

The use of multiple footprints leads to multiple measurements of elevation differences between crater rim and floor. It is a problem of photointerpretation to decide to which surface locations one needs to assign the various peaks of the echo function. The use of these observations permits one to create a refinement of the coarse DEM and represent the shape of the crater in more detail than Figure 3 originally suggested.

[1]The altimeter antenna produces a 30° wide beam. This is sharpened by various techniques to the footprints reported here. However, strong reflectors outside the footprint and within the resolved range may still be recorded and mislead the analysis of the altimeter data.

TABLE 3. OBSERVATION AND MEASUREMENT TECHNIQUES FOR THREE-DIMENSIONAL MAPPING WITH RADAR

Technique	Status in Magellan
Altimetry by profiling	Available in various implementations
Stereoscopic measurements	Initial imagery has inappropriate geometry
Interferometric measurements	Potentially possible at poles
Shadow length measurements	Imaging is at steep look angles, thus no shadows exist
Lay-over measurements	Only useful for vertical objects
Shape-from-shading	Available, but unstable with single images
Using symmetry of an object	Available, simulates "stereo," i.e., a second image, by assuming that the object is symmetrical

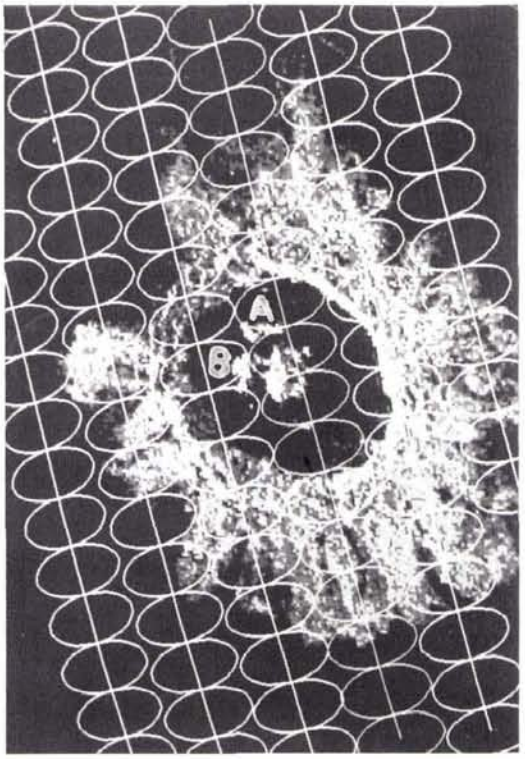

FIG. 4. Image of crater Danilova and superimposed altimeter footprints with a diameter of about 10 km by 15 km. The Crater diameter is about 38 km. The Image covers an area of 150 km by 75 km. Image produced with the MGNDQE Software (Magellan ARCDR Data Quality Evaluation Software, Courtesy P. Ford, MIT).

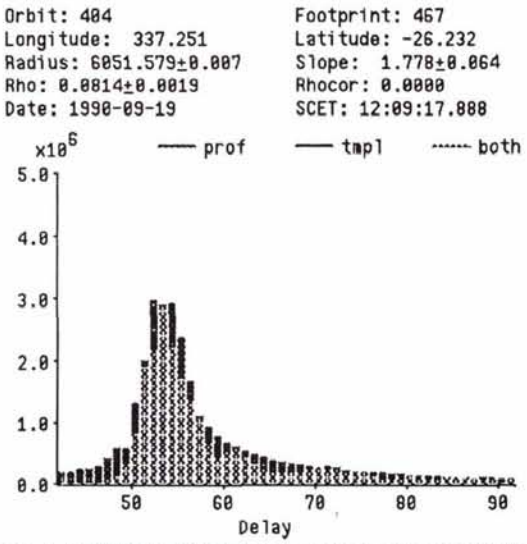

FIG. 5. Individual altimeter trace or echo function from footprint A (see Figure 4). The difficulty exists in allocating the strongest echo (the peak) to a specific location within the footprint. Image produced with the MGNDQE Software (Courtesy P. Ford, MIT).

The accuracy of this approach is dependent on one's ability to allocate the echo peaks to specific terrain locations. This is an error-prone problem. The elevation itself is described with an accuracy defined by the ability to resolve the echo time; Pettengill *et al.* (1991) quote an error of ±5 metres. However, this may not only be contaminated by the ambiguity of the horizontal position of the sources for such peaks, but also by spurious echoes from strong reflectors off to the side.

In summary, we assess the height of the crater rim from three representations of altimetry data:

- straight extraction of the elevations from the global square grid DEM (GDTR);
- reading one elevation off each altimeter footprint and attaching it to the center of the footprint; we denote this method in this report by ARCDR and circumvent the interpolation and filtering process that is used to create the GTDR;
- studying each echo function, relating it to the SAR images and interpreting multiple peaks in the function as reflections off specific surface features (internally denoted as ARCDR+).[2]

We confirm that the best altimetry-based estimate for the height of individual objects requires that the echo function be combined with photointerpretation, as implemented in the third method.

EXPLOITING SYMMETRY

Dalke and McCoy (1968) used opposite-side radar image coverage to compute terrain slopes and elevation differences in a non-stereo mode by using monocular measurements of the length of terrain slopes in two overlapping radar images. Figure 7 illustrates this concept. Through the observed lengths L_1 and L_2 in the two images 1 and 2, one can compute the terrain slope.

Elachi (1990) described a variation of this approach for single images, assuming that the object is symmetric like a crater or volcano. Then one can obtain the two "stereo" images simply by using two segments of the symmetric rim of the crater or symmetric slope of the volcano. This produces the two observations to compute the terrain slope and elevation difference as sketched in Figure 8.

The accuracy of the approach depends on several factors, including the error in identifying the rim and floor of a crater, the error of the assumed incidence angle (Figure 9), the error of measuring the length of the slope (Figure 10) and the lack of symmetry. In the example of crater Danilova we may commit errors of measuring the slope length in the range of ±2 pixels in near range, and of ±6 pixels at the far range. At look angles off-nadir of 34° this will create an uncertainty of ±220 metres in the crater floor-to-rim measurement (Figure 10).

SHAPE-FROM-SHADING

Detailed knowledge of topographic relief at the sensor's pixel resolution supports the study of the terrain's genesis and may help in understanding surface and sub-surface structures. It also reduces ambiguities about surface properties left after studies of reflectivity, emissivity, and roughness. Shape-from-shading or photoclinometry (Wildey, 1986) present the promise of assigning a slope and elevation value to each pixel of a radar image, while modeling the backscatter properties of the imaged surface. The technique exploits the relationship between the strength of a radar return towards an antenna and the inclination of the terrain element towards the antenna. We refer to earlier descriptions of the technique, for example by Thomas *et al.* (1991), who applied it to the refinement of stereoscopically derived elevation data.

Because this method relies on the knowledge of the surface's radar backscatter properties, it would have to be based on an

[2]The Magellan ARCDR Data Quality Evaluation software (MGNDQE) was written at the Massachusetts Institute of Technology to permit analysts to use altimetry in this manner. MGNDQE was employed in this study, courtesy of P. Ford, MIT.

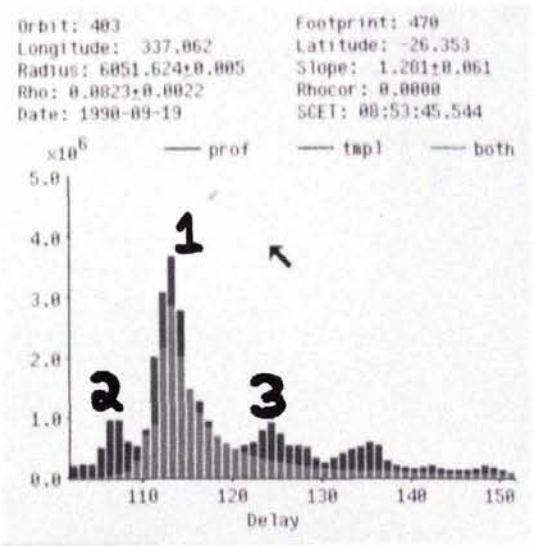

Echo function
Signal strength versus echo time

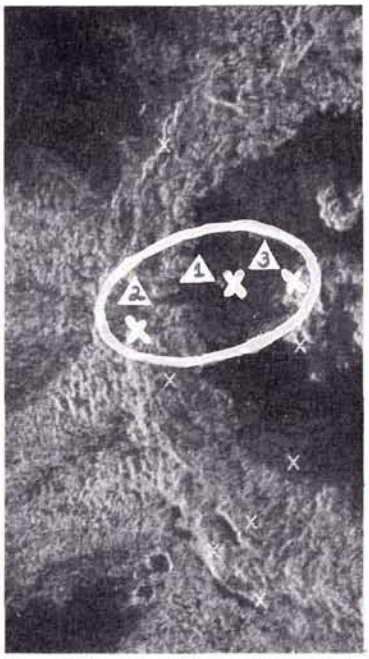

SAR image with Orbit 403,
Footprint 470 - source of echo Peak

FIG. 6. Example of an altimetry echo function over the rim of Crater Danilova, showing multiple echo-peaks indicative of reflections off the rim and crater floor (compare Figure 4). Image produced with the MGNDQE Software (courtesy P. Ford, MIT). Also shown is the detailed SAR image covered by the altimeter footprint, with the result of photointerpretation to allocate peaks of the echo function to specific locations on the SAR image.

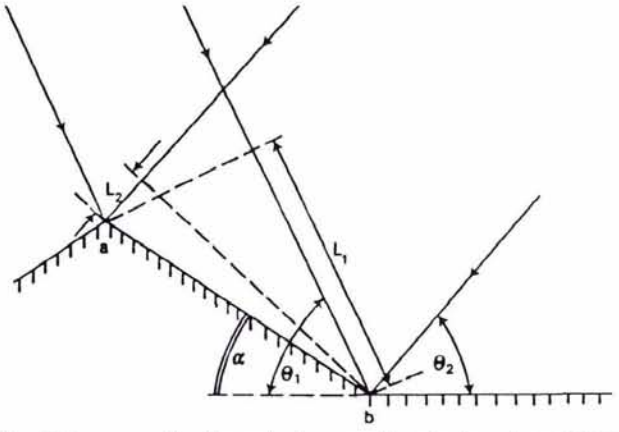

FIG. 7. Two opposite side radar images at two look angles produce the length *ab* of the slope in a slant plane presentation at L_1, L_2. This can be used to compute the terrain slope from measurements of length of the images of the slope (Dalke and McCoy, 1968).

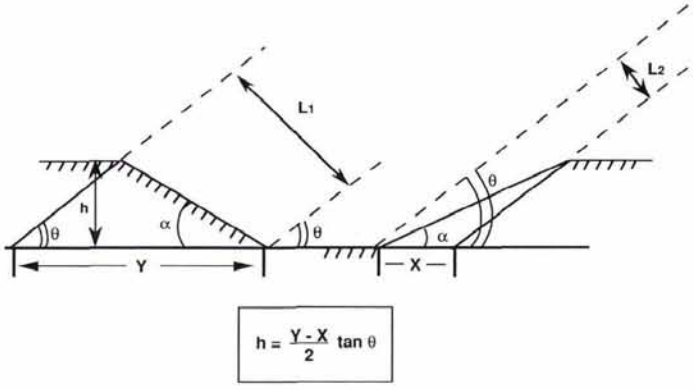

FIG. 8. Variation of the slope measuring technique for single images of symmetric features (Elachi, 1990). Here, L_1, L_2 represent slant range and X, Y a ground range presentation.

independent observation of such backscatter properties at varying incidence angles at each pixel. In the absence of a measurement one employs a default function, e.g., the law by Hagfors (1970), with an estimate of the so-called Hagfors parameter.

Image brightnesses are first converted to terrain slope, then to elevations. The method is expected to be sensitive to error accumulation in the integration of slope values to produce elevation results; elevation errors may be due to incorrect backscatter values or radiometric calibration, as well as noise.

We would prefer to apply the technique to multiple image data sets. In this case the backscatter properties do not necessarily have to be fully known or assumed, but certain parameters can be computed from multiple gray values at each pixel, and the sensitivity to noise is reduced. However, in the initial Magellan coverage, there is hardly any redundancy in the image data sets. Even at 80° North, the incidence angles from overlapping images vary by no more than 0.3° and therefore do not produce the desired multiplicity in observations (see Figure 11 and the later section on Mountainous Area at 83° North).

The technique, and the interpretation of its results, must thus be applied judiciously. The elevation data typically are accurate in a relative sense, i.e., changes of slope and elevation across a short distance of one kilometre or so will be useful. The propagation of slope errors into elevation data, however, can pro-

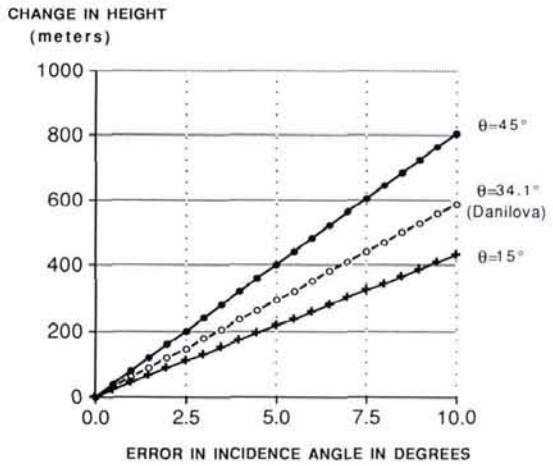

FIG. 9. Errors of the depth/elevation measurement technique of Figure 8, computed for errors of look angles off nadir. Danilova is at 34°.

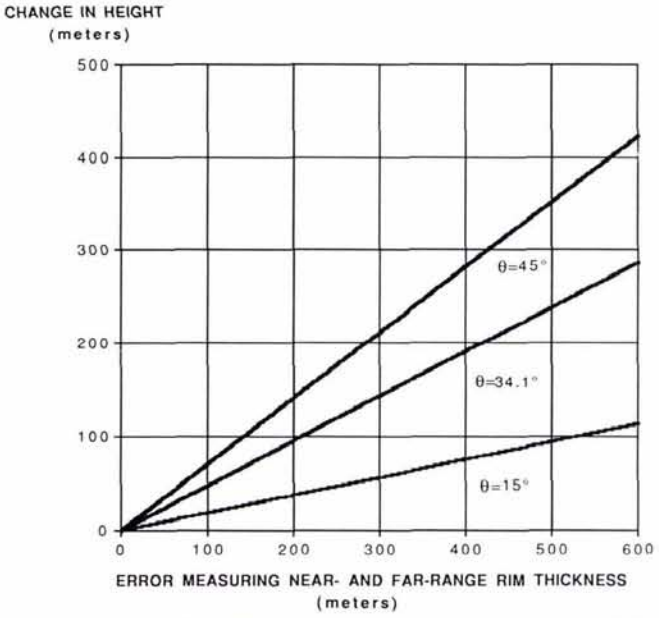

FIG. 10. Errors of the depth/elevation measurement technique of Figure 8, computed for errors of measuring the length of a slope (in metres).

duce significant absolute errors over larger distances between individual pixels. At this time, actual accuracy studies are not available, and the terms "small distance" and "large errors" are poorly defined.

EXAMPLES OF ELEVATION OBSERVATIONS AND DISCUSSION

CRATER DANILOVA

The rim height of crater Danilova (the "depth") was measured with results as summarized in Table 4. All altimetry-based data determine absolute elevations and produce the crater rim height as a difference between absolute measurements. Notable results are the difference in the elevation measurement from altimetry and the symmetry method; and the variation in the floor elevation obtained from various ways of using the alti-

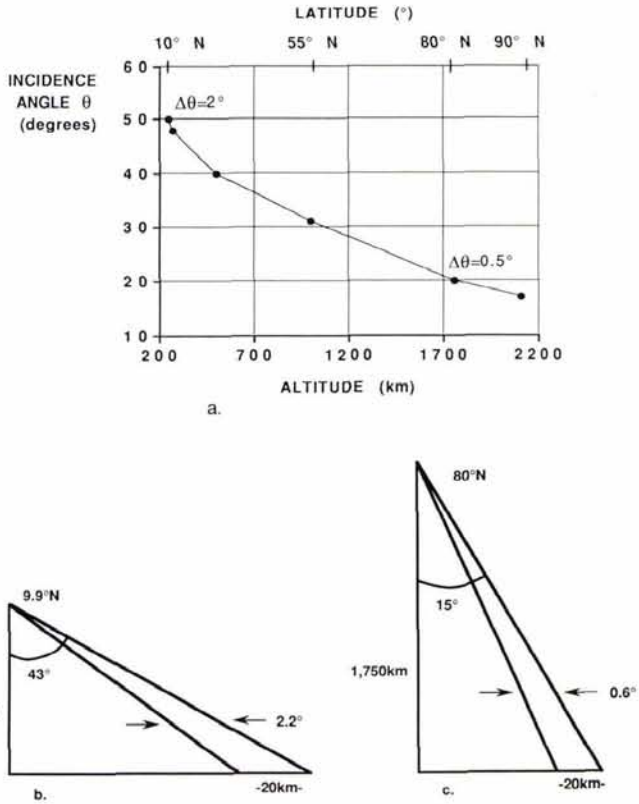

FIG. 11. Approximate look angles off nadir, and variation of look angles within the imaged swath. (a) General graph; (b) At periapsis; (c) At 80° North. Any overlapping images will have differences in incidence angles that are smaller than look angle variations within one swath.

TABLE 4. OBSERVATIONS OF DEPTH OF IMPACT CRATER DANILOVA ON VENUS, OBTAINED FROM DIFFERENT MEASURING AND ANALYSIS TECHNIQUES. ALL VALUES IN METRES, WITH A MEAN VENUSIAN RADIUS OF 6,040 KM SUBTRACTED. "VARIATION" IS THE ROOT-MEAN-SQUARE VARIATION IN THE OBSERVED QUANTITY WHEN USING MULTIPLE OBSERVATIONS AT DIFFERENT LOCATIONS ALONG THE CRATER RIM AND FLOOR. GDTR = GLOBAL TOPOGRAPHIC DATA RECORD, A SQUARE GRID DEM INTERPOLATED AT A GRID SPACING OF 4.5 KM FROM THE ALTIMETER; ARCDR = ALTIMETRIC AND RADIOMETRIC COMPOSITE DATA RECORD, USED TO EXTRACT ONE SINGLE ELEVATION VALUE PER ECHO FUNCTION; ARCDR+ = USE OF ARCDR TO EXTRACT MULTIPLE ELEVATION VALUES PER ECHO FUNCTION EMPLOYING PHOTOINTERPRETATION ON THE SAR IMAGES TO SPECULATE ABOUT THE SOURCES OF MULTIPLE SIGNAL PEAKS IN THE ECHO FUNCTION.

	Elevation of		Variation of Elevation		Crater Depth		Number of
Method	Floor	Rim	Floor	Rim	Value	Variation	Observations
Altimetry GTDR	11,765	11,838	35	24	73	39	7
Altimetry ARCDR	11,597	11,980	38	278	383	236	18
Altimetry ARCDR+	11,221	11,936	292	250	715	390	6
ARCDR+ Max Value	N/A	N/A	---	---	1,345	N/A	1
Symmetry-Technique	N/A	N/A	---	---	1,560	216	7
Shape-from-Shading	N/A	N/A	---	---	1,704	412	20

metry data. Even the refined analysis of altimetry defines crater depth at about 700 metres; the symmetry method results in a measurement of 1,560 metres.

The refined use of altimetry in the method denoted as ARCDR+ led to the independent analysis of six different footprints and echo- functions of pulses covering the crater floor and rim. An example was presented in Figure 6. For the crater floor we obtain three different elevations, depending on how we extract values from the altimeter. We find that the floor's topographic elevation is erroneously "lifted" by a method that analyzes altimetric echo functions automatically and without regard for an interpretation of the terrain based on SAR images.

The variations in all observations within each method are not necessarily measurement "errors," but represent a variation encountered when repeating the observations at various parts of the crater. The variation may thus be a result of errors, or may be caused by an actual variation of crater depth.

Figures 12 through 17 illustrate the results of the methods. In Figure 12 we show the contour lines obtained from the basic altimeter DEM. It illustrates that the crater depth is underestimated. Figure 13 indicates the locations at which the symmetry method was applied to measure crater depth and to refine the altimetry DEM. Figure 14 produces the resulting contour lines. It is evident that the rim and floor of the crater are distinctly reflected in the data sets. A perspective visualization of the DEM from the symmetry method is presented in Figure 15. A comparison with Figure 3 indicates the improvement accomplished in adding the result of the symmetry measurements to the altimeter DEM. Contour lines from the shape-from-shading method are shown in Figure 16 and indicate the degree of morphological detail one can expect in the application of this technique.

Failure to properly adjust radiometric differences in adjacent F- BIDRs leads to a local depression in the Eastern part of the crater floor.

The reconstruction of the shape of the crater by the various observations is further illustrated in Figure 17 with the help of a particular profile through the crater, as produced by each method. The depression in the East part of the crater floor produced by the shape-from-shading method is evident, as is the smoothing of the crater rim by the altimetry-based measurements.

Mountainous Area at 83° North

To illustrate shape-from-shading in an area of the planet where multiple image coverages exist, a data set was processed at 83° North, 335° East. The radar image coverage is shown in Figure 18. Figure 19 presents an example of images as a mosaic of four orbits. A second mosaic was produced from four other orbits to provide multiplicity of inputs. A total of eight such mosaics could be made because at this latitude, each ground point appears in up to eight images. Taking the two with largest differ-

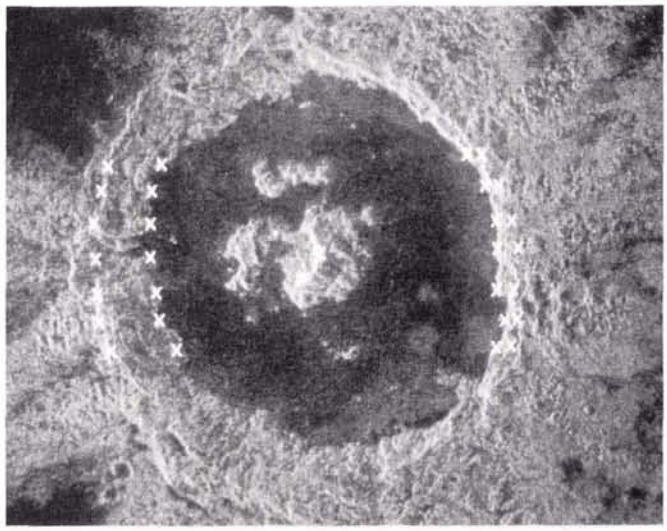

FIG. 13. Crater Danilova and the locations where points were collected along the rim and floor of the crater for application of the symmetry method.

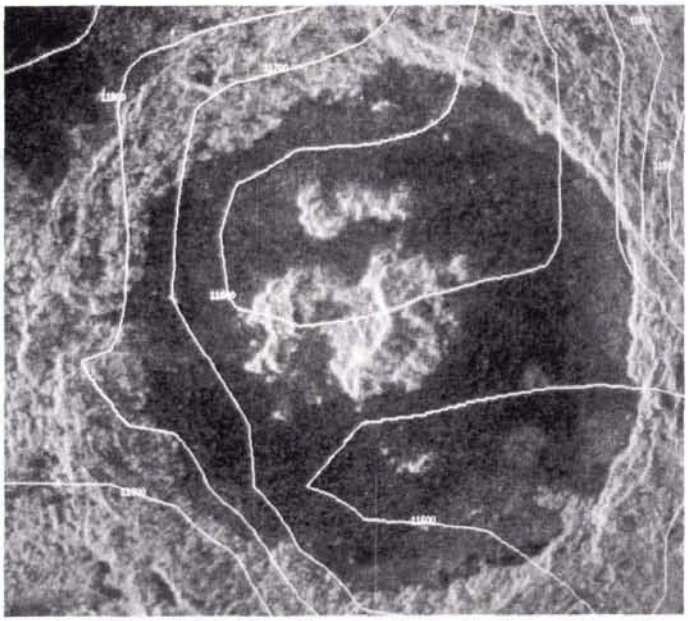

FIG. 12. Contour plot at 100 metres over Crater Danilova, obtained from the standard GTDR-altimetry DEM. Note the lack of correspondence between the contour lines and the apparent terrain shape and the elevation differences of about 200 metres between rim and floor.

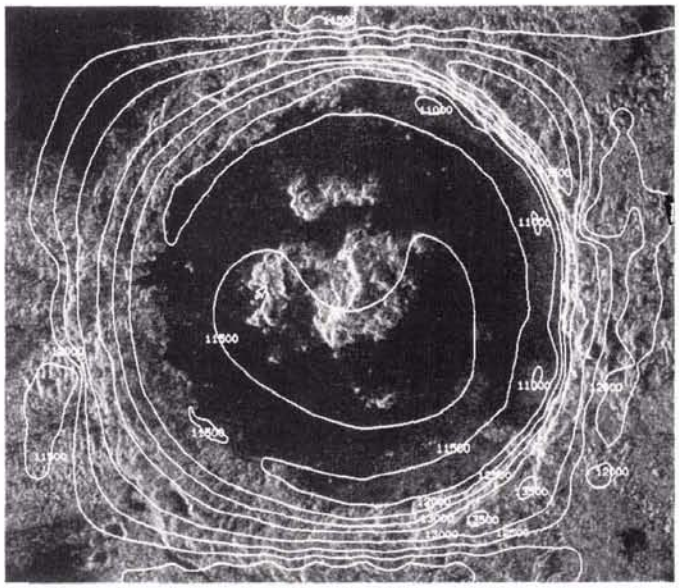

FIG. 14. Contour plot produced from the DEM created from the symmetry method, at 500-metre intervals. The DEM is a combination of the standard GTDR-altimetry DEM and the symmetry method and presents a rim height of 1,500 metres above the floor, and a slope of 21°.

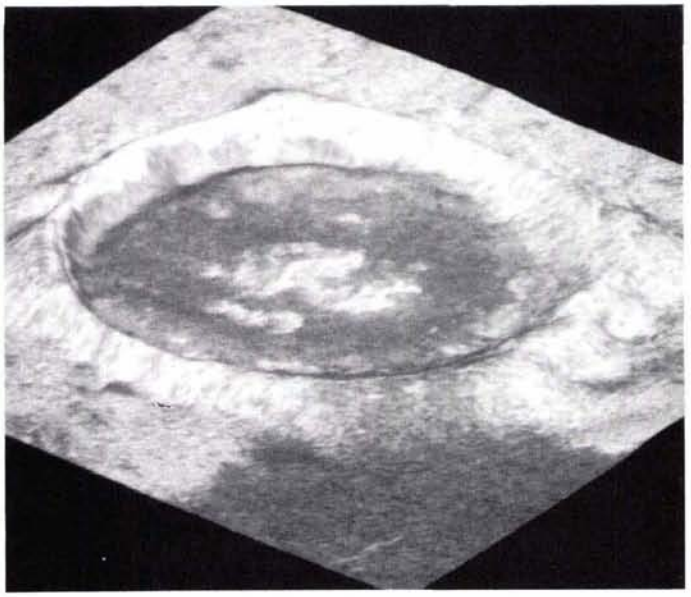

FIG. 15. Perspective view of the elevation model in Figure 14 produced as a combination between standard GTDR-altimetry and measurements with the symmetry method.

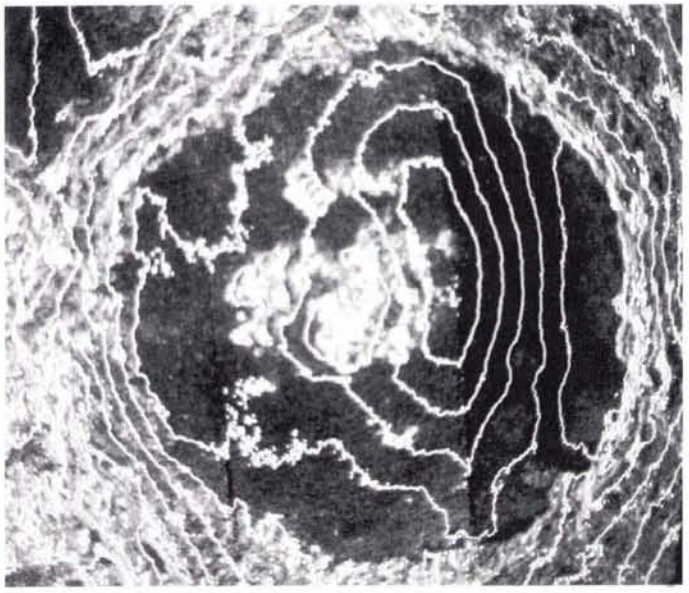

FIG. 16. Contour lines obtained from shape-from-shading. Note the detail in the morphology of the contour lines, and the local depression at the east edge of the floor, resulting from a discrepancy in radiometry between the two rightmost images. Rim slope is 14° to 24° and compares with the slope value for the symmetry method.

ences in look angle still produces a look angle disparity of only 0.3°. The data set does therefore not satisfy the requirement of multiple different images as an input to the shape-from-shading process. However, it permits one to illustrate qualitatively that multiple image shape-from-shading can successfully be processed into terrain elevation data, as illustrated in Figure 20. No quantitative assessment of accuracy is possible at this time because no independent meaningful elevation data set exists for this topographically accentuated area.

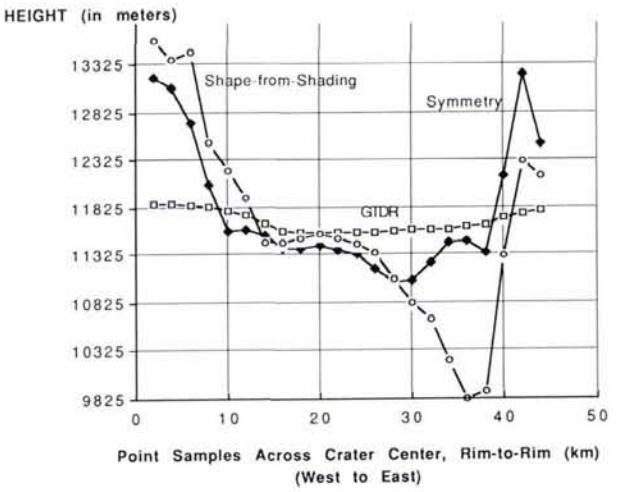

FIG. 17. Set of elevation profiles obtained from various techniques for Crater Danilova.

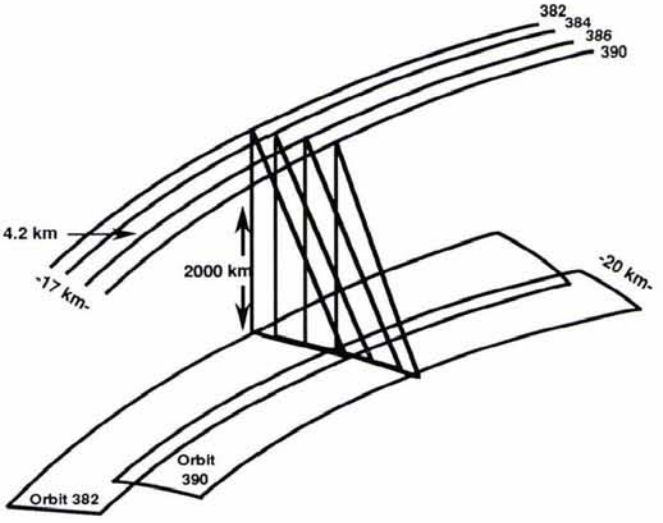

FIG. 18. Imaging geometry at 83°N with multiple overlaps.

CONCLUSIONS AND OUTLOOK

The initial coverage obtained from the Magellan Mission to planet Venus was not designed to support the detailed measurement of terrain shape, elevations and elevation differences. The nominal products of the Mission consist of altimetry observations at a spacing of up to 20 km, and of radar images converted to image mosaics. These are being produced by dead-reckoning based on a satellite ephemeris and topographic model from Pioneer Venus and Venera.

In some well constrained instances, measurements of the third dimension can be obtained for specific terrain features that resolve smaller objects with more detail than is present in the standard product from altimetry. We have described a set of tools for the measurement of elevation data and examined their accuracy. Application of these tools to crater Danilova resulted in some discrepancies between the estimates for the crater's rim height obtained from the altimeter (700 metres) and from a technique that exploits the assumption of symmetry (1,560 metres).

The use of shape-from-shading is obstructed by the fact that only single image coverage is available. This makes it a tool not well suited for the absolute measurement of elevations and which

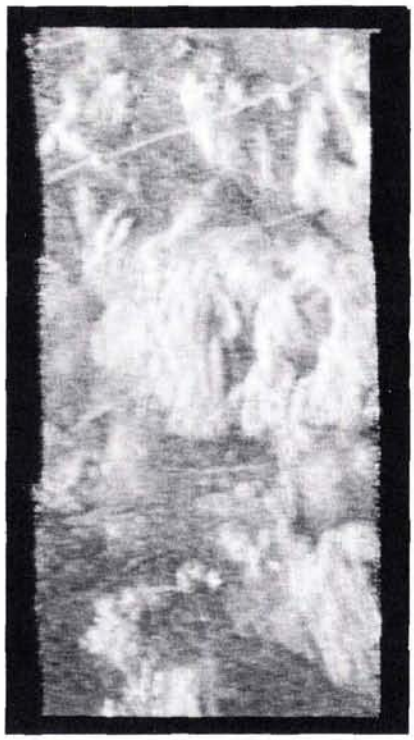

FIG. 19. Image mosaic covering 45 km by 77 km, at a latitude of 83°N, 335°E, consisting of four individual image strips (Orbits 382,384, 386, 390).

FIG. 20. Perspective view of the digital elevation model of the area in Figure 19, produced by shape-from-shading. Draped over the DEM is the image mosaic.

tends to be exaggerated to values that are higher than elevation differences obtained from other methods. However, it lends itself to define the micro-relief by associating a slope value to each pixel. It can thus serve to refine elevation measurements obtained by other means.

All measurement techniques at this time produce results that are not verifiable other then by comparing them to one another. There is no mechanism available to assess and explain the differences and relate them to a known "true" crater rim height. However, we present evidence that altimetry underestimates the height differences between a crater's rim and floor. The example of crater Danilova with a diameter of 38 km is underestimated by 50 percent.

As Magellan enters into the production of a second coverage by radar images at very different look angles, we expect to be able to add new techniques to the tool box for elevation reconstruction, and to employ the techniques described here in a manner that improves their accuracy. We expect to be able to verify the initial statements about elevation differences by comparing them to results from a later coverage, and we believe that multiple images should be combined into stronger solutions.

There exists the opportunity to study images of the North pole of Venus, which is covered in Cycle 1 in every second orbit; the resulting 800 images are taken at varying azimuth angles. This should permit one to solidify one's understanding of some of the analysis issues from multiple images.

ACKNOWLEDGMENTS

We are grateful to Peter Ford (MIT) for his help in understanding altimetry data; to Craig Leff (JPL) for his support in our search through Magellan images; and to Henry Moore (USGS) for providing information on location of geological features.

REFERENCES

Dalke, G., and R. McCoy, 1968. Regional Slopes with Non-Stereo Radar. *Photogrammetric Engineering*, Vol. 34, No. 5, pp. 446–452.

Elachi, C., 1990. Informal Memorandum to the Magellan Radar Investigation Group, Jet Propulsion Laboratory, Pasadena, California.

Hagfors, T., 1970. Remote Probing of the Microwave and Infrared Emissions and Radar, *Radio Science*, Vol. 5, pp. 189–227.

Leberl, F., 1990. *Radargrammetric Image Processing*. Artech House, Norwich, Massachusetts, 600 p.

Pettengill, G., P. Ford, William T.K. Johnson, R. Keith Raney, and Laurence A. Soderblom, 1991. Magellan: Radar Performance and Data Products. *Science*, Vol. 252, pp. 260–265.

Science, 1991. Magellan at Venus, Special Issue, *Science*, Vol. 252, pp. 247–312.

Saunders, R. S., 1990. The Surface of Venus. *Scientific American*, December, pp. 60–65.

Thomas, J., W. Kober, and F. Leberl, 1991. Multiple Image SAR Shape-from-Shading. *Photogrammetric Engineering & Remote Sensing*, Vol. 57, pp. 51–59.

Wildey, R., 1986. Radarclinometry for the Venus Radar Mapper. *Photogrammetric Engineering & Remote Sensing*. Vol. 52, pp. 41–50.

(Received 1 July 1991; accepted 3 July 1991